Key Points:

- The geometry of blocks influences soil distribution around blocks but not the mode of downslope transport on soil mantled hillslopes
- Fragmentation leads to block surfaces appearing less weathered with increasing distance from cliffs
- Block fragmentation along pre-existing fractures can result in a complex distribution of limestone block sizes with distance from the cliff

Correspondence to:

N. R. McCarroll and A. J. A. M. Temme,
nmccarroll13@ksu.edu;
arnaudtemme@ksu.edu

Author Contributions:

Conceptualization: Nicholas R. McCarroll, Arnaud J. A. M. Temme
Formal analysis: Nicholas R. McCarroll
Funding acquisition: Nicholas R. McCarroll
Investigation: Nicholas R. McCarroll
Methodology: Nicholas R. McCarroll
Project Administration: Arnaud J. A. M. Temme
Resources: Arnaud J. A. M. Temme
Supervision: Arnaud J. A. M. Temme
Writing – original draft: Nicholas R. McCarroll
Writing – review & editing: Arnaud J. A. M. Temme

Transport and Weathering of Large Limestone Blocks on Hillslopes in Heterolithic Sedimentary Landscapes

Nicholas R. McCarroll[1,2] and **Arnaud J. A. M. Temme[1]**

[1]Department of Geography and Geospatial Sciences, Kansas State University, Manhattan, KS, USA, [2]Now at Seaton Hall Kansas State University, Manhattan, KS, USA

Abstract Geomorphic transport laws that describe the movement of material across landscapes generally hide the role of lithological and climatic boundary conditions behind proportionality terms. The geomorphic community aims to characterize the role of these boundary conditions and include them in mechanistic transport laws. A more detailed mechanistic understanding is needed for hillslopes formed in heterolithic rock that weathers into weak regolith and hard blocks, such as in hogbacks. The properties of such blocks may determine both the process and rate of their transport downslope. We focused on soil mantled hillslopes in the Flint Hills of Kansas in the United States, where we studied the role of block shape and size under a limestone cliff that breaks up approximately into equal amounts of cubic and tile-shaped clasts. Based on previous studies on the transport of rock clasts, we hypothesized that cubic and tile-shaped blocks should be transported differently, leading to different distributions of size and orientation with increasing distance from the cliff. Block shape does have significant influence over how soil collects and is stored on the hillslope near blocks. Yet, few cubic blocks appear to be transported through tumbling in contrast with assumptions in recent modeling work. We found complex relationships between block size and distance from the cliff face and we propose that this is due to weathering via fragmentation. This process produces discrete smaller fragments from a larger parent block. We suggest that at least in Kansas both cubic and tile-shaped blocks are transported primarily by creep processes.

Plain Language Summary In steep landscapes like those of the Rocky Mountains or the Canyons of the Colorado Plateau, large boulders and blocks move downslope quickly and violently under the force of gravity. Recent research has shown that the general shape of these blocks is important for now they tumble and how far they can travel downhill. However, in much flatter landscapes, like those of the Great Plains, we generally don't have a well-defined understanding of how these large rock blocks move downhill. We hypothesize that blocks that are broadly cubic or tile-shaped will move differently downslope and so should lead to them occupying different positions in these flatter landscapes. Our investigation is focused on the Flint Hills of Kansas. We find in our landscape of soil-covered hills and shallow slopes that all blocks, despite shape, must be transported downslope via a process known as creep. We also find evidence that the blocks on these hills quickly break apart into halves and quarters and this may be helped along by factors such as fire. Our results lead us to believe that block shape is not as an important consideration in downslope movement for landscapes like the Flint Hills.

1. Introduction and Conceptual Framework

Geomorphic transport laws are mathematical relationships that describe the mass flux of material over a landscape. The formulation of such laws is central to the modern field of landscape evolution modeling (Dietrich et al., 2003; Temme et al., 2017; Tucker & Hancock, 2010). Landscape evolution models have been used in constraining sediment fluxes, understanding the developmental history of landscapes, and projecting the evolution of landscapes into the future (Dietrich et al., 2003; Temme et al., 2017; Tucker & Hancock, 2010). Laws have been formulated to describe fluvial erosion in both transport and detachment limited settings, and to simulate the processes related to hillslope diffusion (Braun et al., 2001; Dietrich et al., 2003; Roering et al., 2001), among others. The earliest diffusion transport law was the linear diffusion model, derived from equations describing chemical diffusion (Culling, 1960; Roering et al., 1999). This transport law initiated landscape modeling of hillslope evolution (Culling, 1960; Roering et al., 1999). The linear diffusion model states that the flux of hillslope material is directly proportional to topographic gradient (Culling, 1960; Hirano, 1968). However, this model failed to replicate observations of hillslope curvature in steep landscape positions (Roering et al., 1999). In response to this

shortcoming, the non-linear diffusion model was formulated, which better replicates observed hillslope profiles, yet still lumps processes ranging from creep to landsliding (e.g., Dietrich et al., 2003; Martin, 2000; Roering et al., 1999.). The non-linear model quantifies hillslope regolith flux (q_s) as:

$$q_s = \frac{\mathrm{D}S}{1-(S/S_c)^2}$$

where S is the hillslope gradient, and S_c is a limiting slope steepness beyond which sediment fluxes become infinite (through landsliding). Practically, S_c is often defined as the steepest slope present in a landscape that has reached equilibrium. However, not all steady state landscapes may necessarily attain slope steepness near S_c and so may remain as a theoretical value for low-gradient landscapes. The proportionality parameter D is a constant combining the role of vegetation, lithology, regolith properties, and climate, among others. This collection of many factors into one term can be done to simplify our landscape evolution models. However, this simplification also reveals our knowledge gaps concerning how these factors come together and interact to influence hillslope and sediment transport, thus requires tuning of D to each new studied landscape (e.g., DiBiase et al., 2017; Marston, 2010; Roering et al., 2001).

Climate, lithology, and vegetation cover are known significant controls on the flux of material (e.g., Govers & Poesen, 1998; Marston, 2010; Roering et al., 2001). The geomorphic community has recognized this and is attempting to understand how climate, lithology, and vegetation are reflected in proportionality terms such as D (e.g., Carriere et al., 2020; Johnstone & Hilley, 2015; Pelletier & Rasmussen, 2009). One of the factors that has recently received attention is the lithological composition of the hillslope, particularly in heterolithic settings. The different lithologies in these settings can each produce distinct weathering products with different properties. These properties—grain or clast size, shape, erodibility, and density—can act as controls on material transport (as illustrated for fluvial regimes by Menting et al. (2015)). Of specific interest, the transport of large rock blocks from hard lithologies down a hillslope and into a fluvial channel can significantly modulate erosional signals propagating through a landscape (Duszyński et al., 2017; Glade & Anderson, 2018; Glade et al., 2019; Roth et al., 2020; Shobe et al., 2018, 2021). Therefore, knowing how and when large rock blocks are transported downslope by hillslope processes is important for understanding broader aspects of landscape evolution.

Recent work focusing on hillslope transport of discrete cobble and larger clasts by Duszyński and Migoń (2015), Glade et al. (2017), and DiBiase et al. (2017) has shown that clast size is important in understanding how and at what rates clasts are transported downslope. These studies build upon earlier work beginning in the 1970s examining the transport of large, cobble to boulder-sized, rock fragments downslope (e.g., Govers & Poesen, 1998; Grab et al., 2008; Pérez, 1985; Schumm, 1967; Shobe et al., 2020).

Early work on the movement of rock fragments was done on arid and alpine bare rock slopes (Pérez, 1985; Schumm, 1967). These studies focused on measuring rates of surficial movement of talus material or rock fragments over a finer-grained regolith. Schumm (1967) found that thin, tile-shaped rock fragments are highly mobile on the arid shale slopes of the Colorado Plateau. He proposed that rock fragments on bare regolith slopes move through a combination of sliding, caused by sheet, wash and rafting on creeping regolith. Pérez (1985) observed that talus of varying size and shape on alpine slopes in the Andes moves through a combination of creep driven by temperature fluctuations and needle-ice action. In a similarly arid landscape like the Colorado Plateau, Turkey, Govers and Poesen (1998) showed that dislodging by animals and subsequent rolling can drive downhill clast movement on debris covered slopes. Grab et al. (2008) invokes frost jacking and gelifluction as the primary mover of boulders on slopes in the mountains of New Zealand.

Recent work has established that block size has also emerged as a key control on momentum-based downhill transport and erosional processes. DiBiase et al. (2017) examined the relationship between hillslope topographic roughness and the size of bouncing clasts in steep, soil-poor topographies. They found that when clast size is smaller than the microtopography of the hillslope, the probability of clast interception and storage on the hillslope is high. Caviezel et al. (2021) showed that in steep landscapes dominated by momentum-based transport, block shape has a strong control over movement trajectory: tile-shaped blocks have a greater lateral spread in depositional location at the bottom of steep hillslopes than cubic blocks. However, no examination of these size and shape relationships has been conducted for lower gradient soil-mantled hillslopes.

Glade et al. (2017) observed that ~1 m^3 rock blocks on hillslopes collect soil behind their upslope face, and that blocks had presumably moved in response to significant amounts of hillslope undermining below the block.
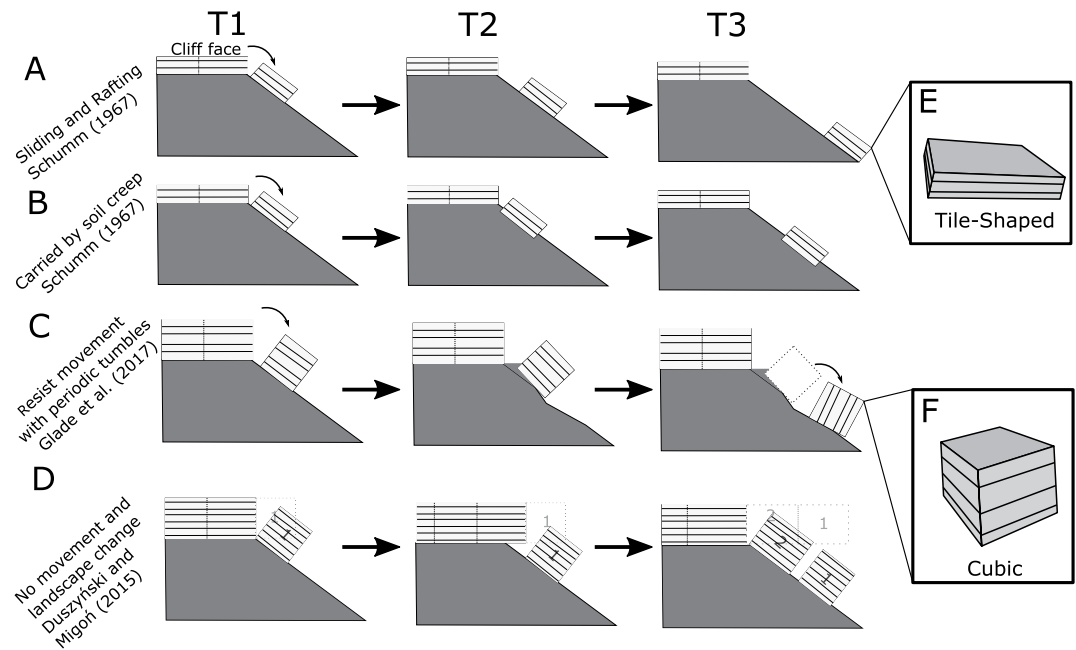
Figure 1. Proposed modes of block movement on hillslopes in literature. Each model is simplified into a three-step progression through time. (a) Block movement rate is faster than soil diffusion due to sliding (Schumm, 1967). (b) Block movement is at the rate of hillslope diffusion and is the result of the block being embedded and transported with the mobile regolith (Schumm, 1967). (c) Blocks resist downslope movement with regolith but are moved through a combination of slope undermining and upslope soil damming resulting in instability and tumbling (Glade et al., 2017). The rate of block movement will be slower than hillslope soil diffusion. (d) Blocks are too large to move and stay where they are deposited (Duszyński & Migoń, 2015). The rate of block movement will be zero. The hillslope around the block lowers and the cliff laterally retreats away resulting in the appearance of downslope block transport. (e) Conceptual example of a tile-shaped block where the long and intermediate axes of the block are much larger than the shortest axis. (f) Conceptual example of a cubic block where the longest, intermediate, and shortest axes are approximately similar in length.

Glade et al. (2017) also observed that the size of blocks produced by hard sedimentary layers systematically decreases in the downslope direction—supposedly through weathering. Based on these field observations, they postulated a resistance of sub-meter and meter-sized rock blocks to the downslope movement of the soil mantle. The implication of that assumption is that the movement of boulder-sized blocks on soil-mantled hillslope is an intermittent process where movement is triggered by undermining of the hillslope beneath the block resulting in blocks that move slower than the mobile regolith.

Duszyński and Migoń (2015) suggested that $\sim 10^3$ m^3 rock blocks, observed in eastern Germany, do not move once they are deposited on a slope below or next to a cliff face, successfully resisting the downslope movement of soil and regolith. In later work, Duszyński et al. (2017) suggested that such blocks, too large to move otherwise, can only be carried downslope passively on mass movements, such as shallow rotational landsliding. This process of landslides carrying massive blocks is a possible explanation for the unexpected position of blocks dozens of meters in length more than 100 m from the cliff face, as observed by Duszyński and Migoń (2015). The research presented above demonstrates the most common mechanisms for moving sub-meter to meter sized blocks downslope are creep, sheet wash-induced sliding, and discrete tumbling, whereas blocks ~ 103 m^3 in size may be transported only through landslide rafting (Figure 1).

Size may not be the only control on the processes regulating a block's movement. Apart from Schumm (1967), who explicitly described the shape of blocks studied, other studies largely observe or assume blocks that are generally cubic in shape. However, based on geometric principles, one should expect the shape to influence mechanisms and rates of downslope block movement. To explore this influence, in this project we simplify block shape into two conceptual categories: cubic and tile-shaped (Figures 1e and 1f).

Glade et al. (2017) proposed that cubic blocks may be rather immobile on slopes except for short intermittent moments of movement. Such cubic blocks, when compared to tile-shaped blocks, have less downward-facing

surface area in contact with the hillslope. Subsequently, the force of swelling hillslope material may be unable to overcome the cubic block's greater pressure, which precludes movement by creep. Instead, movement may primarily result from downslope undermining and slope steepening, causing block instability, tumbling, or sliding (Glade et al., 2017).

On the other hand, tile-shaped blocks as observed by Schumm (1967) are transported in a continuous fashion. Schumm described two primary transport pathways. Tile-shaped blocks can move rapidly via sliding induced by reductions in slope shear strength due to the moisture or surface runoff. Alternatively, tile-shaped blocks can be moved gradually by creep as part of the mobile hillslope regolith. Repeated lifting and lowering related to the periodic shrinking and swelling of material, or frost heave, results in downslope block transport in a similar manner to creep. In either case, tile-shaped blocks appear to be passive actors in downslope transport and depend on the activity of the soil.

The lack of a systematic study on the effect of particle shape or size on downslope block transport in a low gradient soil mantled hillslope setting leads us to ask, "How does block size and shape affect downslope transport as well as soil-block interactions on creep dominated hillslopes?"

To begin answering this research question, we test four hypotheses. These are:

H1: Total block surface area decreases with increasing distance from the cliff face.

H2: Visible signs of surface weathering increase with increasing distance from the cliff face.

H3: Cubic blocks collect soil behind their upslope side, whereas tile-shaped blocks will be surrounded by soil.

H4: The average difference between the slope of a block and the slope of the surrounding hillslope (quantified as Block Relative Slope [BRS]) is large for cube-shaped blocks compared to tile-shaped blocks.

We test these hypotheses in the Flint Hills in north-eastern Kansas. Hard, sub-horizontal limestone layers of the Flint Hills weather into blocks that range in shape from cubes to tiles, and are transported over hillslopes mainly weathered from shale. This property of our study location allows us to examine how the initial properties of large rock fragments, particularly shape and size, affect downslope block transport while controlling for lithology, vegetation, and climate history.

2. Geology and Geography of Study Area

Our research is conducted in the Konza Prairie Biological Station portion of the Flint Hills (39°05′ N, 96°35′ W) outside of Manhattan, KS (Figures 2a and 2b). Konza Prairie spans approximately 35 km² of unplowed tallgrass prairie and has been little modified by humans. The Flint Hills physiographic province (Figure 2a) is approximately 26,000 km² in area and was formed by the erosion of a sequence of quasi-horizontal Permian age limestones and shales (Aber, 1991; Dort, 1987; Oviatt, 1999). The current landscape configuration is estimated to be approximately 2–3 million years old (Frye, 1955; Oviatt, 1999). Evidence of the previous landscape configuration is present as chert-rich hilltop gravels found across the Flint Hills and eastern Kansas. The drainage network that deposited the gravels sourced its material from eastern Colorado and western Kansas and ran primarily in an east-west direction before the establishment of the modern drainage network (Aber, 1997, 2018).

In more recent times, the region has experienced the Pleistocene advance and retreat of glaciers. Glaciers extended into the north-eastern corner of Kansas, at their maximum extent during the pre-Illinoian (~650 ka) glaciation, culminating in the damming of the Kansas River near Wamego, KS and giving rise to Glacial Lake Kaw (Aber, 1991; Balco et al., 2009; Bierman et al., 1999). Our study site is approximately 10 km from the terminal limit of the pre-Illinoian Glaciation (Figure 2a). During the Late Pleistocene and Holocene, valleys and hillslopes in north-eastern Kansas were topologically stable, but responding to climatic changes (Beeton & Mandel, 2011; Layzell & Mandel, 2020; Smith, 1991). For example, the Konza Prairie portion of the Flint Hills experienced stream aggradations and incisions at approximately 8,000, 3,000, and 1,700 yr B.P. (Smith, 1991). The primary stream in Konza, King's Creek, began evacuating material again around 180 yr B.P. and is currently deeply incised into its own alluvium and partially into bedrock. This Holocene history mimics that of other streams in the Flint Hills, such as Fox Creek, which is nearly 100 km south of our study location (Beeton & Mandel, 2011).

The Flint Hills are known for their stairstep hillslope profiles, whose morphology is controlled by alternating layers of quasi-horizontal shale and limestone (Frye, 1955) (Figure 2c). The soft shales form soil-mantled parts of hillslopes, whereas the limestones can form small (up to 2 m high) bedrock ledges and cliffs which contour
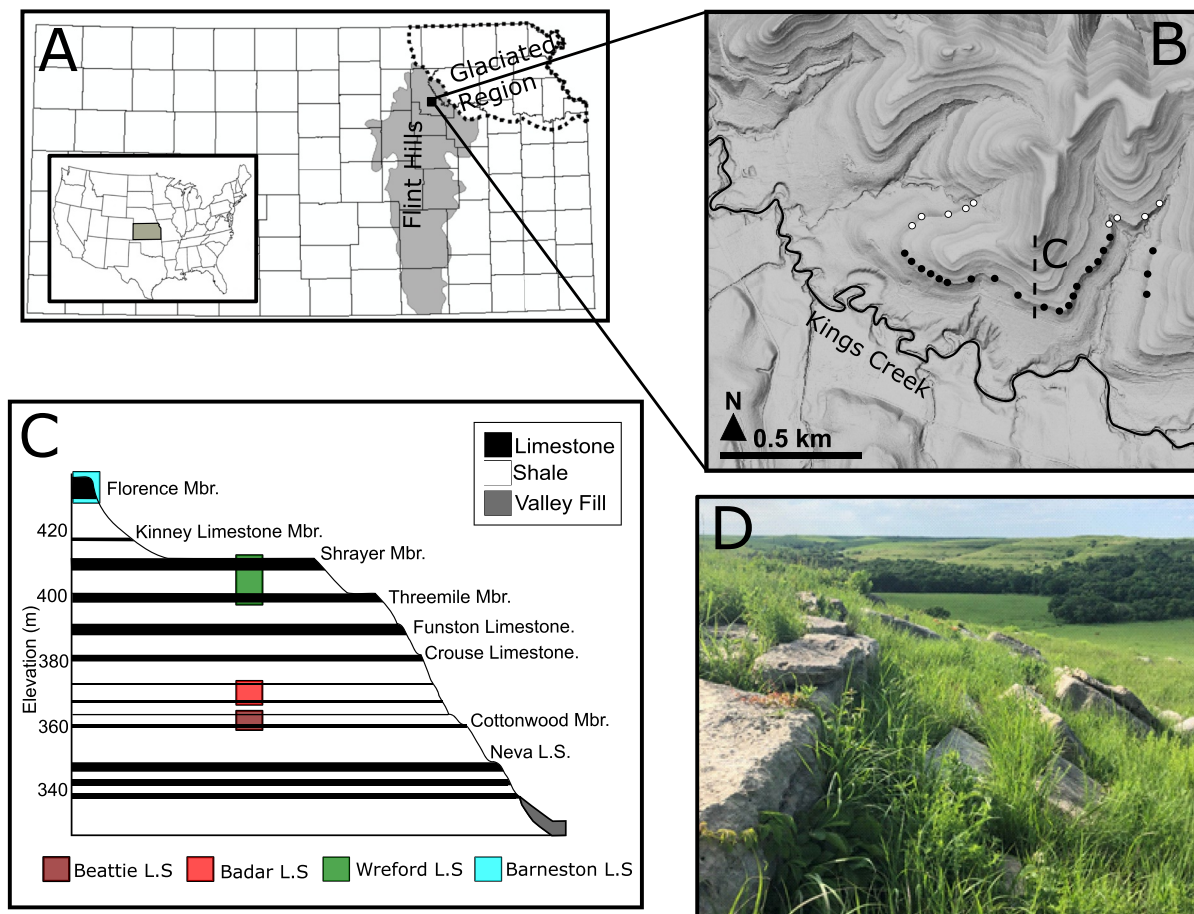
Figure 2. (a) Physiographic provinces of Kansas, the Flint Hills and the Glaciated Region. The location of Konza Prairie is denoted with rectangle. (b) Hillshade map of a small study portion of Konza Prairie demonstrating the characteristic staircase hillslope morphology of the Flint Hills region. Slope block survey locations are denoted with circles. White points represent transects in forest setting; black points represent transects in grassland setting. The major stream in Konza Prairie, Kings Creek, is traced with a solid black line. The dashed line represents typical stair-step hillslope represented in panel (c) which depicts lithologic controls on landscape morphology. (c) Stratigraphic cross-section of the region demonstrating the lithologic control particular limestone units have on landscape morphology. Major bench or cliff forming limestone units are named. Colored regions represent major limestone lithologic units that have been split up into limestone member sub-units. The abbreviation "L.S." represent "limestone," and "Mbr" represents "member." Adapted from Smith (1991) and not to scale. (d) Example of small limestone cliffs formed from Badar Limestone and large rock blocks on slopes common in Konza Prairie, KS. Limestone cliff in left-hand portion of photo is approximately 0.25 m in height and rock is pre-fractured into ~1 × 1 × 0.25 m blocks. Large rock blocks are in center and right-hand portion of photo. Large rock blocks are found up to approximately 10 m downslope.

along the landscape. The benches and cliffs thus primarily run parallel with stream valleys cut by first-order ephemeral streams. Locations where streams cross limestone benches are marked by increases in tree cover and the development of amphitheater hillslope morphology centered on the stream. The cliff-forming limestones are well-fractured into regular units at approximately one-m intervals that eventually form the boulders and blocks that are deposited on the shale slopes below the cliffs (Frye, 1955) (Figure 2d). The blocks vary between cubic and tile-shaped and are assumed to move via tumbling and soil rafting respectively, as hypothesized above.

We studied a prominent limestone bench formed from the Cottonwood Limestone Member of the Beatie Limestone (Aber & Grisafe, 1982; Imbrie et al., 1964) (Figures 2b and 2c). The studied section of cliff mainly faces south and east, with some sections facing north. This limestone unit was primarily chosen due to its prominence in the landscape, with clear vertical separation from the next-higher bench-forming Morrell Limestone. The vertical separation caused the formation of an approximately 50 m long slope, with few to no observable blocks in its lowest 10 m in most locations, which should prevent contamination from Morrell-limestone blocks in the studied part of the hillslope under the Cottonwood Limestone member.

The study cliff formed by the Cottonwood Limestone and the hillslope under it are covered by mostly grassland and some forest. Forested sections are occupied by a combination of trees and dense woody underbrush that
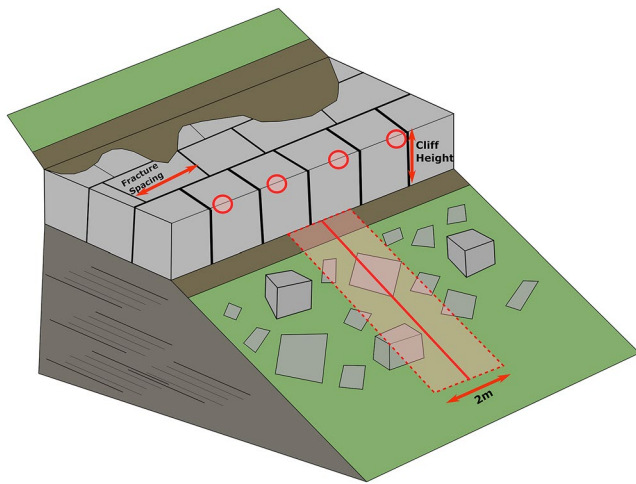
Figure 3. Schematic of slope block transect and cliff measurements. A slope transect is shown as a red line surrounded by the 2 m-wide transect area. Red circles on the cliff face represent where cliff property measurements were taken. Cliff property measurement locations are separated by approximately 2 m. All blocks touching or partially overlapping the transparent red transect survey block were measured.

grow on top of and in the fractures of the cliff face and around the blocks on the hillslope under it. These forests take the form of gallery forests that parallel streams of the region (Knight et al., 1994). Four species of tree, the American Elm (*Ulmus americana*); the Honey Locust (*Gleditsia triacanthos*); the Hackberry (*Celtis occidentalis*); and the Eastern red cedar (*Juniperus virginiana*); account for approximately 90% of the trees in the area (Briggs et al., 2002). Grassland portions are dominated by tall grasses with infrequent large woody plants occupying some cliff face positions. Dominant grass species are big bluestem (*Andropogon gerardii*); Indian grass (*Sorgastrum nutans*); little bluestem (*Schizachyrium scoparius*); and switch grass (*Panicum virgatum*) (Briggs et al., 2002).

3. Methods

Properties of the Cottonwood Limestone cliff and blocks on the hillslopes under it were recorded every approximately 25 m for a 2 km distance along the cliff, excluding locations near trails. This spacing between measurements was implemented to capture spatial variations in cliff properties and in blocks on the underlying slope. Examples of properties of interest include cliff height, bedrock fracture spacing, surface weathering, and block size and shape. This survey scheme resulted in observations from 30 transect locations along the cliff (Figure 2b).

3.1. Cliff Measurements

A set of four cliff measurements were collected for each location separated by 2 m to capture local variability (Figure 3, red circles). Surface weathering of the cliff surface was again visually estimated as the percentage of surface area affected by spalling, flaking, and pitting. Fracture spacing and orientation were recorded in two pairs to reflect the presence of two primary fracture directions and to calculate the size of future blocks before their release. Fracture orientation was measured as an azimuth and fracture spacing was measured as a distance separating one fracture to another (Figure 3). These measurements allowed us to quantify the expected initial dimensions of blocks deposited on hillslopes in this landscape.

3.2. Block Measurements

Block properties were measured for all blocks in a 30 m long, 2 m wide transect straight down the slope from the cliff face formed by the Cottonwood Limestone (Figure 3). Block properties such as size, weathering, and downslope dip were then aggregated over 3 m distance intervals during data analysis. Minimum block size observed was set at 64 mm (corresponding to a 0.004 m^2 surface area). This minimum represents the cutoff between pebble and cobble-sized rock fragments and represents the smallest grain size that can be easily observed in the grassy study location. Distances between all blocks and the overlying cliff were measured along the transect line from the center of the slope block. Block size was recorded as two measurements: the length of the longest and intermediate axes of the block. Each axis was perpendicular to the other. Size was reported as an area calculated by multiplying these two measurements. While we did not measure the short axis of blocks, we did categorize by shape. Blocks that had a short axis <0.5 * intermediate axis were recorded as "tile-shaped" and blocks that have a short axis >0.5 * intermediate and long axis were recorded as "cubic" (Figures 1e and 1f). This distinction was implemented as it best reflected our initial first order field observations and categorization of rock blocks into categories of "cubic" and "tile-shaped." For ease of communication, we continue to use the terms "tile-shaped" and "cubic" when referring to the two shape classes of hillslope blocks in the results and discussion sections. Blocks were designated "undetermined" if this distinction could not be confidently made. This designation was made for 65 of 842 blocks measured.

Weathering state was assessed visually as the percentage of the visible block surface that was occupied by surface pitting or spalling. We recognize that this method may underestimate the surface affected by weathering if spalling has removed large thin flakes that make the new surface look un-weathered. This process of spalling may be a

mechanism by which the surface of these blocks weather through time. Spalling may lead to a decreasing relationship between distance and weathering. However, we do not believe that the process of surface spalling is fast enough to significantly affect the surface of a block that is occupied by pitting. We were not able to observe many instances where large portions of a block surface were reset by spalling. Yet, we acknowledge that our values for surface weathering percentage may be minima controlled by the process of surface spalling.

Block dip in the downhill direction was measured in degrees using a digital inclinometer placed at the center of the block. Hillslope steepness was calculated at a 2 m resolution (derived from a 2 m lidar-derived DEM, Blackmore (2019)). The calculated hillslope steepness was then subtracted from the block dip to obtain a BRS. The azimuth of the surface of each block was calculated from the DEM using aspect of the hillslope at the block position. These observations were collected to quantify spatial relationships that reflect transport processes that could move large blocks downslope.

Additionally, qualitative observations of stability, burial, and embedding were recorded to deduce transport processes. Block stability was recorded as stable or unstable depending on if movement or rotation resulted from the force of a human foot pushing the block. Burial condition was based on how embedded a block was in soil. The perimeter of embedded blocks was probed with either a soil knife or rock hammer to estimate the depth at which the bottom of the block occurred and in extension how much of the block was buried below the soil surface. If at least 50% of the block's short axis was embedded, then a block was described as buried in soil. Blocks that were less than 50% embedded were recorded as unburied. For blocks that were buried, a secondary designation was given based on how the block was embedded. If a block was surrounded by soil, it was recorded as buried on all sides, whereas blocks only buried on the upslope or downslope faces were recorded as such.

4. Results

A total of 30 slope block survey transects were performed, resulting in a total of 842 block observations. Three hundred sixty blocks were cubic and 417 blocks were tile-shaped. A large majority of blocks were in grassland transects (717), while 108 blocks were observed in forest transects. Seventeen blocks were observed in a transitional region between forest and grassland.

4.1. Size, Shape, Weathering

Before release from the cliff, the average block size is 2.12 ± 1.82 m^2. In grassland, pre-release blocks have an average size of 2.07 ± 1.38 m^2, whereas in forest, pre-release blocks have an average area of 2.31 ± 2.66 m^2. These differences between forest and grassland are small and not significant at the 0.05 level. On hillslopes under the cliff, the average size of blocks of both shape classes is 0.39 ± 0.67 m^2. Tile-shaped blocks have an average size of 0.50 ± 0.80 m^2, and cubic blocks have an average size of 0.32 ± 0.56 m^2. This size difference between tile-shaped and cubic blocks is large and significant (t-test, $p < 0.001$). Blocks in forest (0.38 ± 1.11 m^2) are also overall larger than blocks in grassland (0.32 ± 0.50 m^2, t-test, $p < 0.001$), although this difference is less substantial. We report other statistics for block properties in Table 1.

The average BRS for all blocks is $9.00 \pm 10.64°$. This means that there is an average difference between the dip of a block and the steepness of the local hillslope of 9°. The average BRS of tile-shaped and cubic blocks are $8.36 \pm 9.3°$ and $10.16 \pm 12.6°$, respectively. This small difference between them is not significant (t-test $p = 0.08$). In grassland, blocks have an average BRS of $8.65 \pm 10.53°$, whereas in forest, blocks have an average BRS of $9.69 \pm 10.78°$. This difference between forest and grassland is also small and not statistically significant ($p = 0.351$). The average azimuth for hillslope blocks is $203.36 \pm 70.05°$. Grassland blocks have an average azimuth of $198.70 \pm 59.69°$, whereas forest blocks have an average azimuth of $250.60 \pm 101.89°$ (t-test $p < 0.001$). The average azimuth of tile-shaped and cubic blocks is $207.10 \pm 67.30°$ and $203.30 \pm 72.58°$, respectively. Differences on account of block shape are not significant at the 0.05 level.

Cliff face surfaces have an average estimated surface weathering of 30% $\pm$ 12%. The mean value for surface weathering of blocks on slopes under the cliff is substantially lower, at 19.5% $\pm$ 15%. This difference is statistically significant (t-test, $p < 0.001$). Tile-shaped blocks appeared less weathered (17% $\pm$ 14%) than cubic blocks (23% $\pm$ 16%, t-test $p < 0.001$). Large blocks (>1 m^2) appear to be overall more weathered than smaller blocks (<1 m^2) (Figure 4a).

Table 1
Properties of Large Blocks Separated by Block Shape as Well as Vegetation Cover

	All blocks	Cubic blocks	Tile-shaped blocks	Grassland blocks	Forest blocks
	$n = 842$	$n = 360$	$n = 417$	$n = 717$	$n = 108$
Size (m²)					
Average ± SD	0.39 ± 0.67	0.32 ± 0.56	0.50 ± 0.80	0.32 ± 0.55	0.38 ± 1.11
Median	0.17	0.14	0.20	0.14	0.39
Minimum	0.01	0.01	0.01	0.01	0.02
Max	7.20	6.44	7.20	7.20	6.44
Block Relative Slope (Degrees)					
Average ± SD	9.00 ± 10.64	10.16 ± 12.60	8.36 ± 9.30	8.65 ± 10.53	9.69 ± 10.78
Median	6.00	6.52	5.89	5.48	6.86
Minimum	0.00	0.01	0.00	0.00	0.01
Max	82.36	82.36	71.87	82.36	65.01
Azimuth (Degrees)					
Average ± SD	203.36 ± 70.05	207.10 ± 67.30	203.30 ± 72.58	198.70 ± 59.69	250.60 ± 101.89
Median	215	209.50	215.00	215.00	306.00
Minimum	75	75.00	75.00	104.00	75.00
Max	355	355.00	355.00	352.00	355.00
Surface Weathering (% of surface occupied by pitting)					
Average ± SD	19.45 ± 15.54	23.00 ± 16.69	17.08 ± 14.60	17.82 ± 14.58	28.17 ± 17.84
Median	15.00	20.00	15.00	15.00	25.00
Minimum	0.00	0.00	0.00	0.00	1.00
Max	80.00	80	73.00	80.00	80.00

4.2. Changes Downslope

There is a strong and significant decrease in block size with distance from cliff ($b = -0.0002$ m²/m, $p = 0.019$, Figure 4c). There is also a strong and significant linear decrease in total block area when aggregating over 3 m downslope intervals ($b = -0.41$ m²/m, $p < 0.001$) (Figure 4b). Most blocks, 60%, are found within the first 12 m below the cliff face. There appears to be a visual decrease in the maximum block size with increasing distance from the cliff (Figure 4c). When the largest sized blocks for 3-m distance intervals are examined, there is a substantial and significant decrease (Figure 4c) in maximum size and distance ($b = -1.60$ m²/m, $p = 0.02$). This seemingly linear decrease is also present for the 5th ($p < 0.001$), 10th ($p < 0.001$), and 15th ($p < 0.001$) largest rock blocks ($b = -0.71, -0.47, -0.37$ m²/m, respectively). When specific grain size fractions are calculated over 3 m distance intervals (Figure 4d) there is no significant linear trend for the D_{16}, D_{50}, or D_{84} ($b = 3 \times 10^{-4}, 0.003, -0.014$ m²/m respectively) with distance from the cliff ($p = 0.78, 0.10,$ and 0.08 respectively). The average values of these grain size fractions are 0.05 ± 0.02 m², 0.18 ± 0.05 m², 0.63 ± 0.22 m², respectively. Only the largest grain size fraction, D_{95} ($1.3 + -0.5$ m²), has a substantial and significant decreasing size with increasing distance from cliff ($b = -0.46$ m²/m, $p = 0.007$). There is no significant difference between cubic and tile-shaped blocks in terms of decrease in size with distance, and therefore, tile-shaped blocks remain larger than cubic blocks. There is no significant difference between forest and grassland blocks in terms of decrease in size with distance, either.

When lumped into 3 m intervals, no overall trend can be observed between surface weathering and distance from the cliff face for either tile-shaped or cubic blocks (Figure 5a). However, there appears to be a moderate increasing trend for a subset of blocks at distances 9–27 m from the cliff face. In this interval, we observe both cubic and tile-shaped blocks overall increase surface weathering with increasing downslope position. For all distance intervals, the mean surface weathering percentage of both tile-shaped and cubic blocks are substantially below the mean surface weathering of the modern cliff face. In fact, the mean surface weathering percentage for tile-shaped blocks for distance intervals 0–12 m is significantly below the standard deviation of cliff face surface weathering
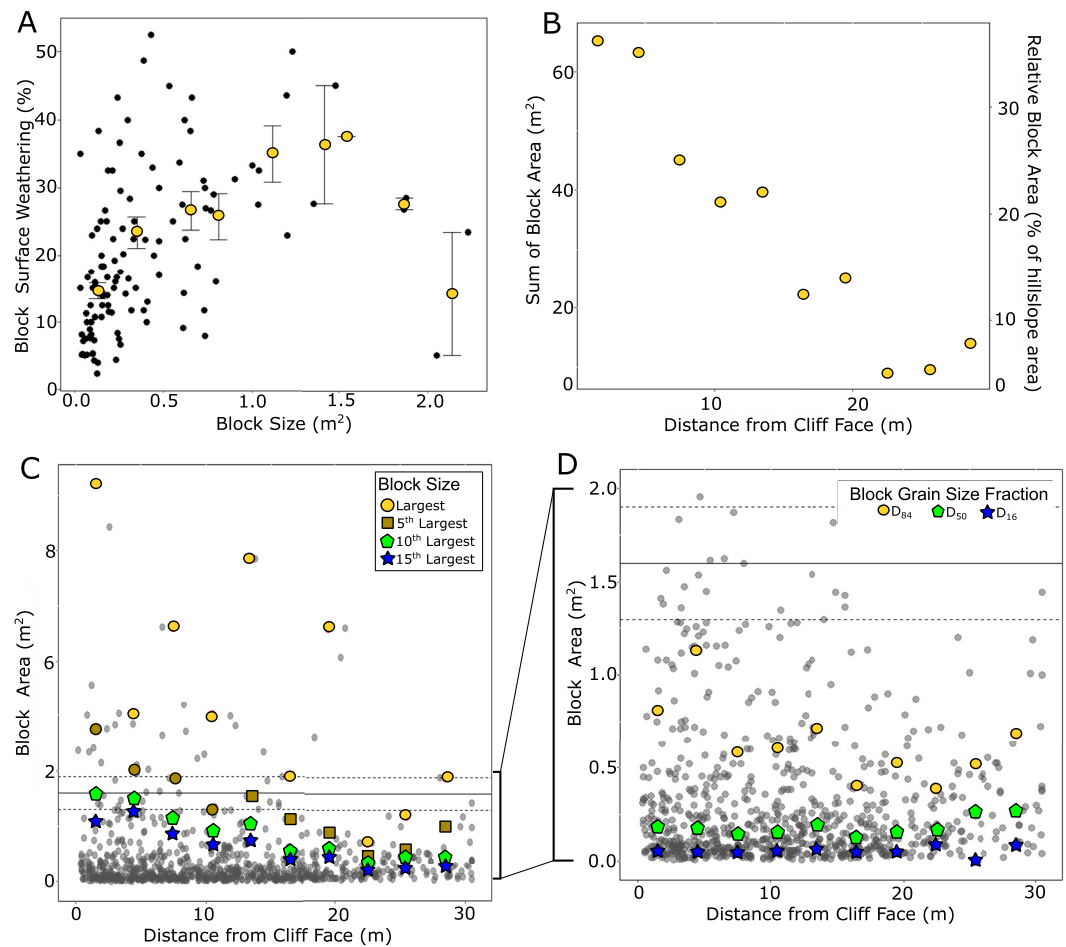
Figure 4. (a) Surface weathering plotted as a function of block size. Yellow points are mean values of distance and weathering calculated at 0.25 m^2 interval. The standard error of surface weathering for each interval is shown with error bars. (b) Sum of block area of hillslope blocks for 3 m intervals. Secondary axis shows the block area as a portion of the hillslope area. (c). Block size as a function of distance for the cliff face. Colored points are the largest blocks in intervals of 3 m to capture trends in surface area on account of block size. The black horizontal line is the median surface area of fractured limestone unit calculated from fracture spacing. Black dashed lines are confidence intervals of the median. (d) Subset of data presented from panel (c), showing block sizes from 0 to 2.0 m^2. Colored points are specific grain size fractions in intervals of 3 m to capture trends in surface area on account of block size. The black horizontal line is the median surface area of fractured limestone unit calculated from fracture spacing. Black dashed lines are confidence intervals of the median.

values. Mean weathering below the standard deviation of cliff face weathering also occurs for distance intervals 15–18 m, and 21–24 m for tile shaped blocks.

All BRS values are greater than zero for both cubic and tile-shaped blocks, reflecting that all blocks are inclined more than the local hillslope. BRS appears to decrease moderately for both cubic and tile-shaped blocks with downslope distance from the cliff face (Figure 5b). Blocks in the first 3 m downslope from the cliff face have an average BRS of 11°, whereas those furthest from the cliff have an average BRS of 3°. This difference is significant (t-test, $p < 0.001$). This signal is present for both tile-shaped and cubic blocks: tile-shaped blocks in the first 3 m of the cliff face have a BRS of 11.1° compared to those furthest from the cliff with a value of 3.8° (t-test, $p < 0.001$) and cubic blocks in the first 3 m of the cliff face have a BRS of 12.5° compared to those furthest from the cliff with a value of 3.9° (t-test, $p = 0.001$). There is no substantial or significant relationship between azimuth and BRS or between azimuth and surface weathering for the entire data set or for tiles and cubes separately.

Shape is not related to block position on hillslopes: there is no significant difference between cubic and tile-shaped blocks in relation to position (two-sample Kolmogorov-Smirnov test, $p = 0.91$, Figure 5c). Unstable and stable blocks also appear to be in about the same position on slopes, with slightly more unstable than stable
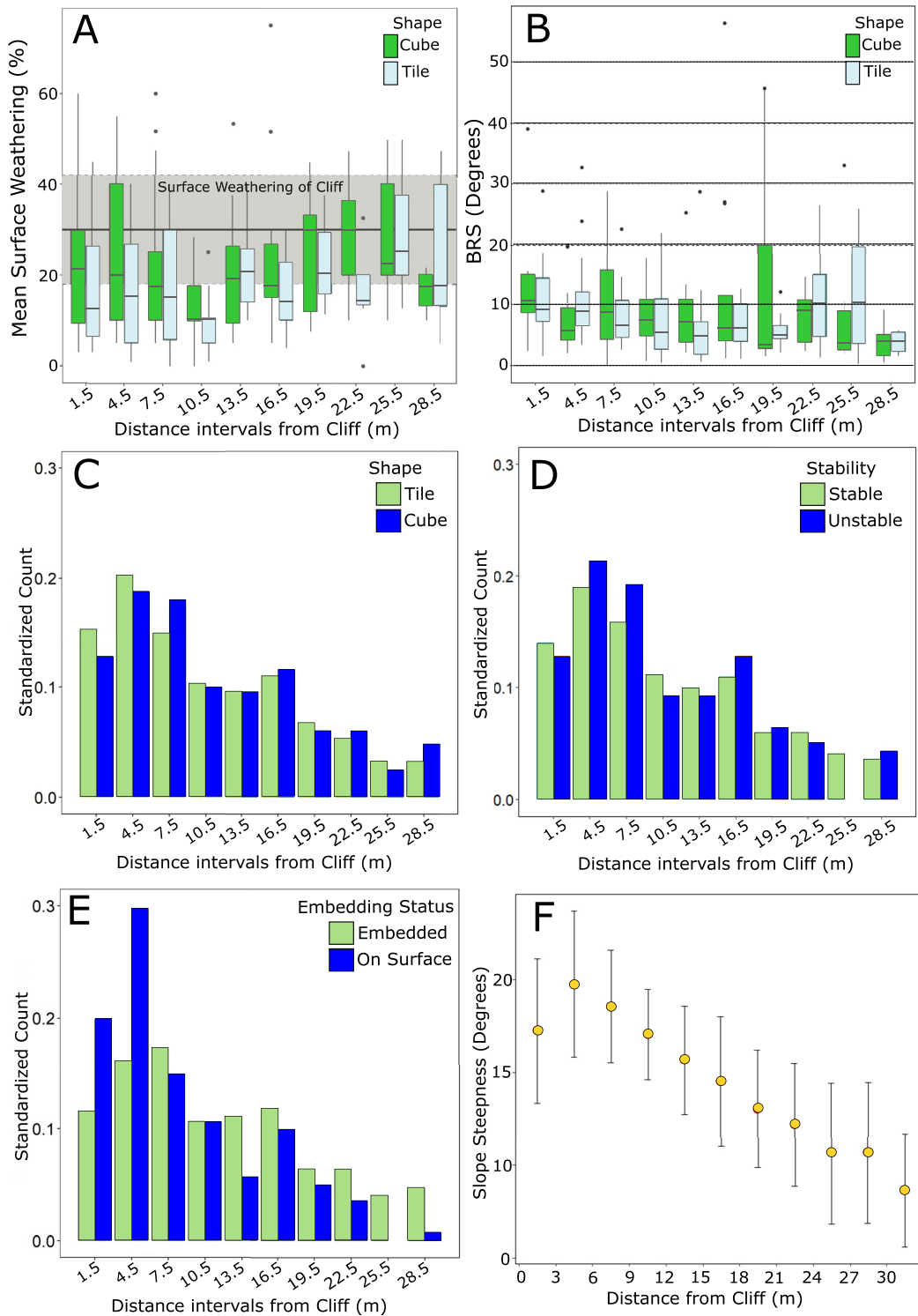
Figure 5.

blocks in the 3–9 m range ($p = 0.65$, Figure 5d). There is no overall significant difference in distribution of blocks that are embedded in the soil or sitting on the surface (Kolmogorov-Smirnov test, $p = 0.41$), there are substantial differences between embedded and on surface blocks in cliff proximal positions (0–6 m from the cliff face (Figure 5e).
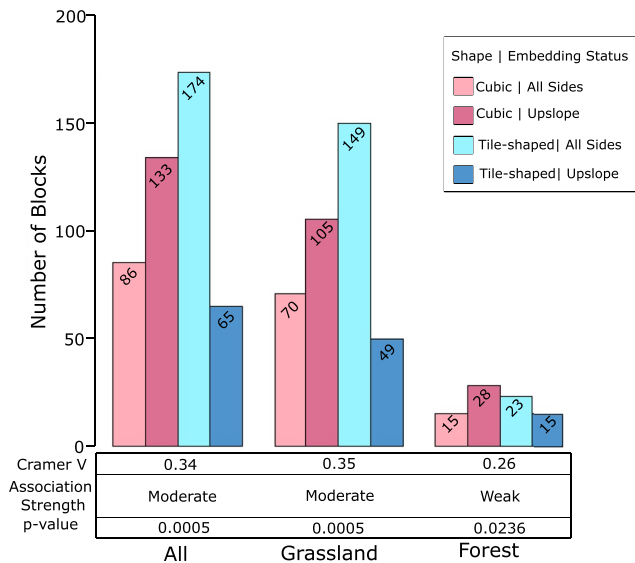
Figure 6. Association analysis results between embedding status and block shape. Results are reported for all blocks measured and then separated out by vegetation cover type. The Cramer V test produces an output between 0 and 1, where 0 is no association, and any value that is above 0.5 is considered a strong association. Associations between 0.3 and 0.5 are moderate strength. Associations below 0.3 are weak associations. This histogram visualizes data used in each combination of block shape and embedding status classes.

4.3. Interaction With Soil

Most blocks (543, or 64%) were embedded in the hillslope soil to some degree. Three hundred eleven blocks were surrounded by soil, 202 had soil only behind the upslope face, and 30 had soil covering only the downslope face. We used a χ^2 test to determine whether block shape and the type of embedding are related for all blocks, for grassland blocks, and for forest blocks (Figure 6). The null hypothesis for this test is that shape and embedding status are independent. This hypothesis was rejected ($p < 0.001$): there is a relationship between block shape and how the block is embedded in hillslope soil. Cubic blocks have more individuals embedded in soil only on the upslope side. Tile-shaped blocks are more often embedded in the soil on all sides. The strength of the association between embedding type and block shape, expressed as Cramer's V, is 0.33, indicating moderate associations for the entire data set (Figure 6). For blocks in forest locations, Cramer's V is 0.25 (low association strength), while in grassland locations, Cramer's V is 0.34 (moderate association strength).

5. Discussion

5.1. Block Size and Surface Weathering

Results clearly show that blocks are decreasing in size through time via weathering processes as they move downslope. There is also a significant decrease in total block size with distance from the cliff face, leading us to accept our first main hypothesis. We further observe that the size of the largest individual blocks (D_{95}, and the largest, 5th, 10th, and 15th largest blocks) decreases with distance from the cliff. For semi-arid and arid landscapes, Glade et al. (2017) and McGrath et al. (2013) observed a logarithmic decrease in size with distance for the largest particles on the hillslopes. For our landscape, we do not find this to be true. Instead, we find that for the largest size fractions decrease in size linearly (linear and logarithmic regression results can be found in Table S1 in Supporting Information S1). We propose these trends reflect the fundamental nature of chemical and physical weathering of limestone blocks in this landscape. As a limestone fragment breaks apart and dissolves, the surface area continues to increase relative to the total block volume. This increase in the ratio between surface area and volume through time corresponds with an increase in weathering which would manifest as a continual decrease in block size. If this is the case, we would expect to see a continual decrease in size along the hillslope toposequence, which we observe here in our data.

We also share Glade et al. (2017) observation that the smallest particle fraction (D_{16}) remains constant across slope positions. This relationship holds true for a significant portion of our observed clast sizes. However, where Glade et al. (2017) interpreted the constancy of the smallest grainsize fraction (D_{16}) as evidence of the constant provision of weathered fragments of larger blocks, we suggest that in our case the stable D_{16} of blocks more strongly reflects the minimum observable rock size more than a physical process. In our study, we did not observe rock fragments smaller than a cobble due to visibility problems in the dense grassy vegetation. This measurement scheme results in an artificial minimum block size that is related to methodology rather than a physical minimum. As a result, we proceed cautiously when making interpretations concerning the smallest grain sizes in our data set. However, the overall implication of block size changes along the topo-sequence remains, weathering reduces block size.

Figure 5. (a) Box plot of average surface weathering of hillslope blocks for 30 slope transects in 3 m intervals. Solid black horizontal line is the average surface weathering of cliff face surfaces via pitting. The dashed black line is the standard deviation of average surface pitting of cliff faces. Each bin of the histograms represents a 3 m interval downslope from the cliff face. To better compare cubic and tile-shape block spatial patterns on hillslopes, the number of individual blocks in each bin has been standardized. Standardization was done by dividing number of points in the bin by the total number of tile-shaped or cubic blocks respectively. (b) Box plot of difference between hillslope blocks and hillslope slope for 30 slope transects for 3 m intervals. Horizontal dashed lines mark 10° increments of Block Relative Slope. (c) Histogram showing distribution of cubic and tile-shaped blocks on slopes. (d) Histogram showing the distribution of stability of blocks on slope. (e) Histogram showing burial status of blocks on slopes. Significant peak of unburied, surface blocks in distance interval 3–6 m. (f) Average hillslope slope profile was calculated from slope values extracted every 3 m along transect survey lines. Average slope value for each distance interval along transects lines is plotted with its standard deviation. The pattern of the data reflects the concave-up hillslope morphology common to hillslopes below this limestone layer.
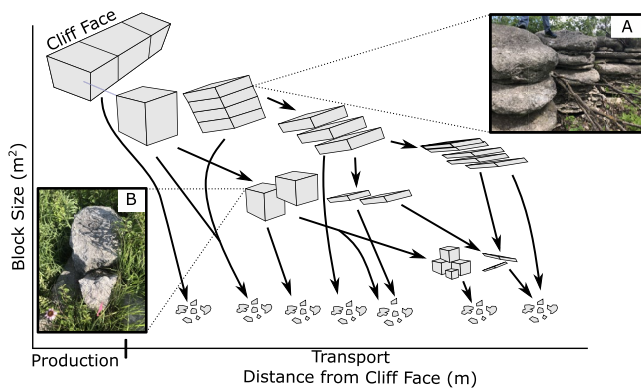
Figure 7. Generalized conceptual pathways of blocks fragmentation. Tile-shaped blocks will maintain or slowly decrease in area whereas cubic blocks will decrease in area as they break apart along a vertical face. Irregular rock fragments along the bottom represent the smallest rock fragment sizes observed. These smallest fragments can have tile or cubic shapes. Fragmentation is always occurring, resulting in small fragments at all distance intervals from the hillslope. (a) Photograph of limestone block breaking along pre-existing horizontal planes. These are blocks that are still part of, or just disconnected from the cliff face. (b) Photograph of limestone block breaking along vertical irregular weakness of crack. Block in photograph is approximately 3–6 m from the modern cliff face.

At the same time, we do not observe a significant increase in signs of surface weathering with increasing distance from the cliff, leading us to reject our second main hypothesis. Our initial assumption that limestone blocks weather primarily via flaking and dissolution of small fragments from the surface would have led to increasing signs of surface weathering on the blocks as they move downslope and become smaller. In keeping with that hypothesis, it also seemed reasonable to expect that blocks would inherit the surface weathering that accumulated when they were part of the cliff face. If that would have been the case, we would expect average block surface weathering near the average cliff surface weathering in cliff proximal positions (Figure 5a). We would also expect that in cliff distal positions the block surface weathering would be greater than the average cliff surface weathering. In contrast to both of those expectations, we see that in cliff proximal positions block surfaces are less weathered than cliff faces. Only at more distal hillslope positions does block weathering begin to increase again and becomes closer to the average cliff weathering. To explain why we do find smaller blocks but not more signs of weathering, we propose that fragmentation into discrete fragments drives a reduction in total block size, produces complex size-distance patterns, and creates new unweathered block surfaces along fracture planes.

Fragmentation is the process by which large clast break up into discrete smaller fractional portions of the original (Wells et al., 2008). This process has most recently been described by Román-Sánchez et al. (2019) who present two broad conceptual fragmentation pathways. In the first broad pathway, particles break into discrete halves, thirds, quarters, and so on. In the second broad pathway, larger particles break off significantly smaller particles and decrease slightly in size themselves. We expected the latter in Konza (through spalling), but our observations point to some combination of the two, favoring the former model. As the largest blocks weather via fragmentation and are transported downslope, they decrease in size (Figures 4c and 7), losing portions of themselves as small fragments or larger discrete daughter blocks. The presence of both types of fragmentation also results in the complex size-distance patterns observed on these hillslopes (Figures 4c and 4d). Yet, when sum together the size of individual rock fragments and large blocks in the downslope direction (Figure 4b) we see a strong linearly decreasing relationship in total block size. This trend would reflect that while the largest block present may decrease with distance from the cliff face, a decreasing proportion of the original large block is preserved on the hillslope. Some of the original material of these large blocks is permanently lost through dissolution or fragmentation to a grain size that cannot be differentiated from the mobile regolith (Figure 4b). This clear relationship is a significant result, as it reflects fundamental landscape relationship between the rate at which large blocks break apart and the rate at which these discrete fragments are transported downslope.

We also observe that most blocks, even in positions very close to the cliff face, are substantially smaller and less weathered than the average and median of limestone fracture spacing. This suggests that substantial fragmentation occurs immediately upon release of limestone blocks onto the hillslope, creating fresh non-weathered surfaces on daughter blocks. This is supported by visual field observations of blocks that have broken apart and are resting directly on the hillslope surface (Figures 2d and 5e) in response to slumping, falling, or tumbling from their cliff face positions. If blocks do indeed have a high likelihood of instant break-up, it would help explain why there is not a significant decrease in block size with distance from the cliff for most size fractions of blocks—the largest decrease has already occurred before the block has moved away from the cliff face. Fragmentation into few large fragments can explain both the absent increase in surface weathering with increasing distance from the cliff (Figure 7) and the fact that blocks are overall less weathered than the average cliff face by providing a process that creates new, unweathered block surfaces. This process can also explain the roughly positive relationship between surface weathering and block size (Figure 4a)—larger blocks have had more time to accumulate signs of surface weathering, whereas smaller blocks are mostly fragmentation products with newly exposed surfaces.

Finally, fragmentation into few, relatively large new blocks can explain the observation that tile-shaped blocks have larger average areas than cubic blocks. We propose that the limestone that forms the slope blocks can break apart in two styles. On one hand, large blocks can break apart into a series of large regular tile-shaped blocks

along horizontal weaknesses, resulting from original sedimentary layering (Figure 7a). This mode of break-up would preserve the large surface formed by the largest and intermediate axes of the parent block and create equally large un-weathered surfaces, thus depressing the observed surface weathering of tile-shaped blocks. On the other hand, blocks can break apart into more cubic halves, quarters, thirds, and so on, breaking along cracks that may have formed after the block separated from the cliff face (Figure 7b). This style of fragmentation would create new cubic blocks with a smaller surface area than the parent block, but fewer new un-weathered surfaces.

As a result of the findings discussed above we propose fragmentation of large blocks into a small number of smaller blocks provides a simple explanation for the complex observed relationships between block size and distance (Figures 4c and 4d). It also provides a simple explanation for the absent relationship between block weathering and distance (Figure 4a). Finally, the difference in style of block break-up discussed above explains why we observe tile-shaped blocks that are less weathered yet larger than cubic blocks (Figure 7).

5.2. Transport and Block Shape

We hypothesized based on previous work by Schumm (1967), Glade et al. (2017), Glade and Anderson (2018), and Caviezel et al. (2021) that different block shapes result in different transport mechanisms. This difference would be caused by block geometry controlling the block center of gravity as well as the volume of soil that can collect behind it. We do indeed observe a similar process of upslope soil collection and downslope soil depletion with cubic blocks (Figure 6), as proposed by Glade et al. (2017). On the other hand, soil builds up equally along all sides of tile-shaped blocks. This shows that block shape plays an important role in how soil is stored on and routed down hillslopes. Thus, we accept our third hypothesis—there is indeed a significant correlation between the shape of a block and the distribution of hillslope material around a block. However, our observations subsequently do not support a different transport process for different shapes.

If cubic blocks would have transported via slow tumbling or rotation, we should have observed overall greater values of BRS. For a cubic block undergoing rotational movement, we would expect surfaces to occupy inclinations ranging from parallel to the slope to nearly standing on edge. Cubic blocks would occupy these high inclinations before tumbling or rotating would happen when a block's center of gravity moves beyond its lower edge. This would result in BRS values that would range from 0° to 25°, assuming a hillslope of 20°. However, this was not observed; both tile-shaped and cubic blocks have similar, low BRS values between 5° and 15°, while hillslope steepness ranges from 20° to 10° (Figures 5b and 5f). Thus, we reject our fourth hypothesis. Instead, we propose that both cubic and tile-shaped blocks are mainly transported by soil creep, as first proposed by Schumm (1967) for substantially smaller tile-shaped clasts in arid settings.

Nonetheless, blocks on occasion do tumble downslope. This tumbling occurs in locations near cliffs where slope steepness is highest (around 20°, Figure 5f). In the field near cliffs, we observe meter and sub-meter scale blocks that are unstable and not embedded in the hillslope in these locations (Figures 5d and 5e). The number of not-embedded blocks reaches its peak in the first 12 m of slopes and so may indicate more recent or frequent movement in this zone (Figure 5e). We also observe that BRS in this region (Figure 5b), specifically in the first 9 m, is at its highest, which suggests an increased likelihood of unstable spatial configurations for a small number of blocks on steeper hillslopes. Recent movement is consistent with the low percentage of surfaces presenting evidence of weathering so close to the cliff (Figure 5a). Our interpretation is that in this cliff-proximal zone, slopes are steeper, and the likelihood of especially newly- or recently released blocks rotating or tumbling is higher, leading to more fragmentation via breakage, exposure of fresh surfaces, and blocks sitting directly on the hillslope surface rather than being embedded in the soil. Furthermore, we propose that the small amount of rotation seen for all blocks (Figure 5b) is most likely related to downslope soil mining and upslope soil storage as proposed by Glade et al. (2017). While we see evidence of rotation related to this process, we do not see evidence of the ultimate effect of downslope movement. This may be due to this landscape not being steep enough to allow for sporadic movement, but rather slight surface rotation while creep processes move the blocks downslope like a conveyor belt.

Further work focusing on whether and how large blocks break apart because of tumbling should be done to confirm or refute these suggestions as well as the mechanism that produces the small amounts of rotation for all blocks. This future work would also need to consider lithologic characteristics that allow for easier break up of some blocks over others. Carbonate rocks in this region as covered above have relatively regular fractures

and joints that generally control the dimensions of the block that is first deposited on the hillslope. We also observe in the field that there is lateral variation in thickness of bedding in the Cottonwood limestone (Aber & Grisafe, 1982). These bedding planes act as a primary weakness that the rock may break along once the block detaches from the cliff face (Dredge, 1992; Ruedrich et al., 2011). We may expect a higher proportion of tile-shaped blocks below cliff locations with thinner beds and thus more bedding planes along which failures can occur. Another lithologic characteristic of interest may be the level of dolomitization of the rock. Carbonate rocks in the region have undergone levels of conversion from limestone to dolostone that can vary laterally (Imbrie et al., 1964). Dolomite has a higher tensile strength (5–25 mPa) than calcite (1–15 mPa) and is less reactive to chemical weathering (Baykasoğlu et al., 2008; Drever, 1982; Paronuzzi & Serafini, 2009; Szramek et al., 2011). In places where the cliff face is composed of more dolomite, we would expect slope blocks to be larger compared to blocks sourced from purely limestone cliffs. This difference would arise due to dolomite's comparatively greater "toughness" to both physical and chemical weathering.

5.3. Effects of Vegetation Cover

While not one of the initial goals of this research, we found that there is a significant size difference between blocks under forest cover and blocks under grassland (Table 1 and Figure S1 in Supporting Information S1). Blocks in forest cover are slightly larger (0.38 ± 1.11) than grassland blocks (0.32 ± 0.55), and the difference is statistically significant (t-test, $p < 0.001$). The difference cannot be attributed to a difference in pre-release fractured bedrock between grassland (2.07 ± 1.38 m^2) and forest sections (2.31 ± 2.66 m^2) of the limestone cliff—there is no significant difference between the two (t-test, $p = 0.63$). Furthermore, while there is a significant difference in hillslope gradients between forest and grassland (t-test, $p = 0.005$), it is not substantial with average hillslope gradients being 17.6 ± 7.1° and 16.5 ± 9.7°, respectively. Therefore, we tentatively reject differences in hillslope gradient as a possible reason for differences in block size between the two vegetation cover types. Interestingly, we also observe a difference in block surface weathering between the two vegetation cover types (Table 1). The surface weathering of blocks is higher in the forest (28.17% ± 17.84%) than in the grassland areas (17.84% ± 14.58%, t-test, $p < 0.001$). This difference in surface weathering suggests the observed differences in size may be the result of differential rates of weathering between the land cover types. We explore below three other possible reasons for the block size difference.

First, block size difference could result from differences in long term fire-related processes between forest and grassland. Grasslands have about three times more intense and energetic fires than forests (Gomes et al., 2020). These differences in fire intensities can lead to stronger physical weathering (through fragmentation and spalling) and thus to smaller blocks in grasslands. This explanation requires that the forest-grassland transition has been spatially largely constant over block-weathering timescales, which we assume to be at least centuries. Indeed, prairie grasses have dominated this portion of the Great Plains region since at least 30,000 yr B.P. (Axelrod, 1985; Johnson et al., 2007; McLauchlan et al., 2013). Over this period, the spatial extend of forests has been primarily contained to areas near stream and river channels (Axelrod, 1985; Knight et al., 1994). Over shorter timescales, the gallery forests expand and contract based on factors such as water availability or grazing patterns, but never reach into higher hillslopes (Knight et al., 1994). Along with the relative spatial stability of the grassland-forest boundary, wildfires have had a significant presence in these grassland landscapes over both human and geomorphic time scales (Gorynski & Mandel, 2009). Fire has been shown to weaken rocks and increase post-fire susceptibility to weathering (Goudie et al., 1992). Micro-cracks can form through individual grains within a rock in response to fire heating, creating new internal weaknesses (Dorn, 2003), which can then lead to macro-scale fractures, breaks, and exfoliation (Dorn, 2003; Goudie et al., 1992; Shtober-Zisu & Wittenberg, 2021). In the context of our landscape, increased fire related weathering in grassland vegetation cover could therefore result in faster rates of fragmentation and increased amounts of fresh surfaces being exposed compared to forest settings. This difference in fire intensity between grasslands and forest could be one explanation for differences in surface weathering as well as block size between the vegetation cover types.

Second, the block-size difference may be the result of landcover-associated microclimatic variations (Eppes & Keanini, 2017; McFadden et al., 2005). Globally, except for the boreal regions, forests dampen the diurnal temperature range that is experienced in a location (Duveiller et al., 2018; Lee et al., 2011). Trees in forested locations shade blocks from direct sunlight, reducing thermal expansion and contraction cycles and thus limiting physical weathering. Due to differential amounts of thermal expansion due to microclimatic controls, the rate of

spalling and fragmentation would be lower in forest settings (Eppes & Keanini, 2017). This lower rate of forest fragmentation would result in slower block breakup, larger blocks, and less fresh surface being exposed compared to the grassland locations.

Third, the observed difference may be the result of leaf litter cover in forested areas covering and obscuring smaller blocks that would be exposed and therefore observed in the grassland setting. However, it is difficult to validate this hypothesis without removing the leaf litter and vegetation.

Further research focusing on the role of microclimate, vegetation shielding, and fire frequency in relation to block weathering in grasslands will be needed to test these propositions. Of the three proposed explanations, we believe that wildfire differences may be the best supported by previous research and be the easiest to investigate. Monitoring the post fire evolution of cracks and fractures that may develop in a block (i.e., Goudie et al., 1992) may be the simplest way to measure resulting differences between forest and grassland fires. However, that still does not give us an insight into crack formation during the fire event itself. Therefore, it may be advantageous to monitor crack propagation during a fire event. For example, the installation of geophones on select large hillslope blocks may allow us to "hear" the cracking as it takes place. Doing this in both forest and grassland settings may allow us to establish differences in fracture propagation intensity for the two different wildfire types. The Konza Prairie research station would be an optimal location to perform this future work due to regular prescribed burns of both forested and grassland locations as well as the bed rock geology that allow the targeting of large blocks of the same lithology for this monitoring.

5.4. Block Transport Mechanisms

Topography, specifically slope steepness, must be a first order control over block transport. Transport of blocks and clasts over hillslopes in very steep mountain settings is primarily driven by the pull of gravity (Caviezel et al., 2021; DiBiase et al., 2017). Yet, in landscapes where hillslope gradients are lower, such momentum-based transport will be rare. However, even on less steep slopes, it stands to reason that block transport via soil inter-action and block rotation increases with slope steepness, and that transport through rotation becomes harder on flatter slopes. In our study location, the slopes below limestone cliff are on average 15°, and we find little evidence of rotational-based transport. We expect that undercutting and rotation-based transport may be observable or even dominant in steeper settings. Steeper slopes increase the potential for rotation-based movement and transport. Furthermore, based on our findings, shape does not have a particularly strong control over the type of mechanism moving blocks downslope in the Flint Hills as opposed to steep landscapes (i.e., Caviezel et al., 2021). Regardless of block geometry, transport occurs mainly along with the mobile regolith via creep.

In addition, we postulate that seasonal temperature and moisture fluctuations are important in determining whether creep processes can move blocks downslope. Grab et al. (2008) showed that in alpine regions, frost jacking and gelifluction can be a primary movement driver of large meter-scale blocks on soil-mantled hillslopes. This type of strongly frost-driven transport occurs irrespective of clay content of the soil (Grab et al., 2008). In less extreme climatic conditions, we could expect that frequent formation and melting of frost in the near surface may be able to repeatedly lift and lower blocks, resulting in movement in the downslope direction in a similar manner as creep. Locations where winters are wet and frequent temperature fluctuations from above to below freezing occur would maximize this type of process's contribution to transport. The climate of our study location may not be ideal for maximizing the cycles of lifting and lowering blocks due to its temperate mid-continental climate characterized by cold, dry winters and warm, wet summers. Most of the precipitation (75%) falls during the agricultural growing season, May through September (Hayden, 1998). However, autumn and spring diurnal temperature swings from above to below freezing coupled with precipitation or substantial soil moisture may result in some amount of lift-ing and lowering over the course of a year due to near surface frost formation. A fair test of the role of climate in frost-jacking transport of large blocks would be possible by finding a climatic gradient along which other conditions remain approximately equal. An example would be examining hillslope blocks below a cliff forming unit that runs along climatic gradient where frost formation frequency decreases. Reduction in frost formation would result in decreased creep efficiency, resulting in more transport being accomplished by slope steepening and tumbling rather than creep. We could perhaps also expect that the frequency of blocks would be lower near cliff proximal positions in climatic conditions where creep is efficient enough to carry away the blocks from the cliff face in northern locations.

A final factor that we believe contributes to creep transport of blocks is the proportion of expansive clays that compose hillslope soils. When clays (especially expansive 2:1 clays such as smectite and vermiculite) wet, they

expand and can cause soil heave. In extreme settings where soils are nearly entirely composed of these 2:1 clays, this swelling can result in damage to building foundations (Kalantari, 2012). This process can lead to lateral movement of slope blocks sitting on top of the soil, rather than rotating or tumbling. Repeated expansions and contractions over time would result in slow downslope movement, just as with frost heave. In experimental settings, a bentonite expansive clay exerted a maximum swelling pressure between 1,000 and 2,500 kPa when wetted (Bhanwariwal & Ravi, 2021). A cubic 1 m^3 limestone block of $\rho = 2,000$ kg/m^3 with 1 m^2 surface area would exert merely 20 kPa of downward force on the soil surface, much less than that of the experiment's pure bentonite. Clearly, in natural settings, the force exerted by swelling clays would be less because clay percentages are lower; many clays are less expansive than bentonite, and expansion can to some extent happen in directions other than upward. Yet, a role for clay-expansion in block transport via creep seems warranted. In our study location, hillslope soils form primarily from upland loess and the shale that form the hillslopes which result in high proportions of silt and clay. Furthermore, as the limestones of our landscape weather, they too release clays as the calcite around them eventually dissolves away.

6. Conclusions

Rock blocks on hillslopes under cliffs in Konza Prairie appear to display complex relationships between size and distance from the modern cliff face. We find that the larger size fraction of blocks exhibits a clear decrease in size with distance from the cliff; however, the relationship is less clear for smaller block sizes. Furthermore, we observe a clear decrease in total block size with increasing downslope distance from the cliff when the size of individual blocks is summed together in 3 m intervals. The sum of hillslope block size for these 3 m intervals does appear to decrease with distance strongly linearly (Figure 4b). We propose that fragmentation of large blocks is a simple explanation for the weak relationship between block size and distance from cliff for moderate and small blocks. Field observations lead us to conclude that the process of fragmentation differs between cubic and tile-shaped blocks leading to tile-shaped blocks being larger in size and less weathered compared to cubic blocks. When these observations are considered together, we conclude that in this temperate mid-continental landscape limestone blocks weather primarily through fragmentation. Furthermore, this process occurs while the block moves downslope through time.

We also find that block shape may play and important role in how soil is spatially distributed around large hillslope blocks. Cubic blocks are more likely to collect soil on their upslope side and act as repositories of soil, whereas tile-shaped blocks are surrounded on all sides by soil, suggesting that soil may move around them more easily. Yet, block shape does not appear to play as important a role in block transport as expected at the beginning of our investigation. We show that most blocks, regardless of three-dimensional geometry, are transported in a fashion first described by Schumm (1967)—on top of moving regolith with creep. This conclusion is based on the following observations: we find on similar values of relative slopes for both tile-shaped and cubic blocks as well as both shape classes having nearly the same distribution of hillslope positions.

Finally, we observe that differences in slope block size and surface weathering is related to differences in vegetation cover types. We suggest that this difference may be caused by microclimatic as well as wildfire intensity differences between grassland and forest vegetation cover. Wildfires can weaken rock and speed up the process of fragmentation, whereas microclimate differences can affect weathering rates. However, further research will be needed to decide between the relative importance of these two possible reasons.

Data Availability Statement

The data for this research is available through the online portal of the Konza Prairie Long-Term Ecological Research (LTER) Program that is managed by Kansas State University and The Nature Conservancy. The Konza Prairie LTER makes available to the public all data associated will research performed at the Konza Prairie Biological Research Station. The Konza Prairie LTER is a comprehensive ecological research, education and outreach program, centered on one of the most productive grasslands in North America. The data can be accessed upon request through the Konza Prarie LTER data portal or at: LTER EDI, https://portal.edireposi-tory.org/nis/mapbrowse?packageid=knb-lter-knz.158.1, Mccarroll and Temme (2022), https://doi.org/10.6073/pasta/65f917edea2318f7f7d63ae4239091c3. This data is a collection of point observations and measurements of large rock fragments on grassland hillslopes. Data was collected from 30 hillslope transects that extend downslope

perpendicular from the bedrock cliff formed from the Cottonwood limestone. Transects are 30 m long and 1 m wide. Observations of blocks include properties such as size, shape, and surface weathering as well as transect head location. This data set also includes observations of cliff properties associated with each transect location. Measurements we made in field by hand for rock fragments larger than a pebble (>64 mm).

References

Aber, J. S. (1991). The glaciation of northeastern Kansas. *Boreas*, *20*(4), 297–314. https://doi.org/10.1111/j.1502-3885.1991.tb00282.x

Aber, J. S. (1997). Chert gravel and Neogene drainage in east-central Kansas. *Current Research in Earth Sciences, Kansas Geological Survey Bulletin*, *240*, 29–41. https://doi.org/10.17161/cres.v0i240.11776

Aber, J. S. (2018). Upland chert gravel in the Emporia, Kansas vicinity: New exposures, observations, and stratigraphic review. *Transactions of the Kansas Academy of Science*, *121*(1–2), 103–110. https://doi.org/10.1660/062.121.0211

Aber, S. W., & Grisafe, D. A. (1982). *Petrographic characteristics of Kansas building limestones* (Vol. 224). Kansas Geological Survey.

Axelrod, D. I. (1985). Rise of the grassland biome, central North America. *The Botanical Review*, *51*(2), 163–201. https://doi.org/10.1007/BF02861083

Balco, G., Briner, J., Finkel, R. C., Rayburn, J. A., Ridge, J. C., & Schaefer, J. M. (2009). Regional beryllium-10 production rate calibration for late-glacial northeastern North America. *Quaternary Geochronology*, *4*(2), 93–107. https://doi.org/10.1016/j.quageo.2008.09.001

Baykasoğlu, A., Güllü, H., Çanakçı, H., & Özbakır, L. (2008). Prediction of compressive and tensile strength of limestone via genetic programming. *Expert Systems with Applications*, *35*(1), 111–123. https://doi.org/10.1016/j.eswa.2007.06.006

Beeton, J. M., & Mandel, R. D. (2011). Soils and late-Quaternary landscape evolution in the Cottonwood River basin, east-central Kansas: Implications for archaeological research. *Geoarchaeology*, *26*(5), 693–723. https://doi.org/10.1002/gea.20367

Bhanwariwal, K., & Ravi, K. (2021). Laboratory swell pressure determination of expansive clays. In *Ground improvement techniques* (pp. 310–315). Springer.

Bierman, P. R., Marsella, K. A., Patterson, C., Davis, P. T., & Caffee, M. (1999). Mid-Pleistocene cosmogenic minimum-age limits for pre-Wisconsinan glacial surfaces in southwestern Minnesota and southern Baffin Island: A multiple nuclide approach. *Geomorphology*, *27*(1), 25–39. https://doi.org/10.1016/S0169-555X(98)00088-9

Blackmore, P. (2019). *GIS20 GIS coverages defining Konza elevations*. Environmental Data Initiative. https://doi.org/10.6073/pasta/f11596621709ba6e4ac48e9f2e898a7a

Braun, J., Heimsath, A. M., & Chappell, J. (2001). Sediment transport mechanisms on soil-mantled hillslopes. *Geology*, *29*(8), 683–686. https://doi.org/10.1130/0091-7613(2001)029<0683:STMOSM>2.0.CO;2

Briggs, J. M., Knapp, A. K., & Brock, B. L. (2002). Expansion of woody plants in tallgrass prairie: A fifteen-year study of fire and fire-grazing interactions. *The American Midland Naturalist*, *147*(2), 287–294. https://doi.org/10.1674/0003-0031(2002)147[0287:eowpit]2.0.co;2

Carriere, A., Le Bouteiller, C., Tucker, G. E., Klotz, S., & Naaim, M. (2020). Impact of vegetation on erosion: Insights from the calibration and test of a landscape evolution model in alpine badland catchments. *Earth Surface Processes and Landforms*, *45*(5), 1085–1099. https://doi.org/10.1002/esp.4741

Caviezel, A., Ringenbach, A., Demmel, S. E., Dinneen, C. E., Krebs, N., Bühler, Y., et al. (2021). The relevance of rock shape over mass—Implications for rockfall hazard assessments. *Nature Communications*, *12*(1), 5546. https://doi.org/10.1038/s41467-021-25794-y

Culling, W. E. H. (1960). Analytical theory of erosion. *The Journal of Geology*, *68*(3), 336–344. https://doi.org/10.1086/626663

DiBiase, R. A., Lamb, M. P., Ganti, V., & Booth, A. M. (2017). Slope, grain size, and roughness controls on dry sediment transport and storage on steep hillslopes. *Journal of Geophysical Research: Earth Surface*, *122*(4), 941–960. https://doi.org/10.1002/2016JF003970

Dietrich, W. E., Bellugi, D. G., Sklar, L. S., Stock, J. D., Heimsath, A. M., & Roering, J. J. (2003). Geomorphic transport laws for predicting landscape form and dynamics. *Geophysical Monograph-American Geophysical Union*, *135*, 103–132. https://doi.org/10.1029/135GM09

Dorn, R. I. (2003). Boulder weathering and erosion associated with a wildfire, Sierra Ancha Mountains, Arizona. *Geomorphology*, *55*(1), 155–171. https://doi.org/10.1016/S0169-555X(03)00138-7

Dort, W., Jr. (1987). Type descriptions for Kansas River terrace. In *Quaternary environments of Kansas* (pp. 103–107). Kansas Geological Survey. Retrieved from http://129.237.140.42/Publications/Bulletins/GB5/Dort2/

Dredge, L. A. (1992). Breakup of limestone bedrock by frost shattering and chemical weathering, eastern Canadian Arctic. *Arctic and Alpine Research*, *24*(4), 314. https://doi.org/10.2307/1551286

Drever, J. I. (1982). *The geochemistry of natural waters*. Prentice- Hall.

Duszyński, F., Jancewicz, K., Kasprzak, M., & Migoń, P. (2017). The role of landslides in downslope transport of caprock-derived boulders in sedimentary tablelands, Stołowe Mts, SW Poland. *Geomorphology*, *295*, 84–101. https://doi.org/10.1016/j.geomorph.2017.06.016

Duszyński, F., & Migoń, P. (2015). Boulder aprons indicate long-term gradual and non-catastrophic evolution of cliffed escarpments, Stołowe Mts, Poland. *Geomorphology*, *250*, 63–77. https://doi.org/10.1016/j.geomorph.2015.08.007

Duveiller, G., Hooker, J., & Cescatti, A. (2018). The mark of vegetation change on Earth's surface energy balance. *Nature Communications*, *9*(1), 679. https://doi.org/10.1038/s41467-017-02810-8

Eppes, M. C., & Keanini, R. (2017). Mechanical weathering and rock erosion by climate-dependent subcritical cracking. *Reviews of Geophysics*, *55*(2), 470–508. https://doi.org/10.1002/2017rg000557

Frye, J. C. (1955). The erosional history of the Flint Hills. *Transactions of the Kansas Academy of Science*, *58*(1), 79–86. https://doi.org/10.2307/3625588

Glade, R. C., & Anderson, R. S. (2018). Quasi-steady evolution of hillslopes in layered landscapes: An analytic approach. *Journal of Geophysical Research: Earth Surface*, *123*(1), 26–45. https://doi.org/10.1002/2017JF004466

Glade, R. C., Anderson, R. S., & Tucker, G. E. (2017). Block-controlled hillslope form and persistence of topography in rocky landscapes. *Geology*, *45*(4), 311–314. https://doi.org/10.1130/G38665.1

Glade, R. C., Shobe, C. M., Anderson, R. S., & Tucker, G. E. (2019). Canyon shape and erosion dynamics governed by channel-hillslope feedbacks. *Geology*, *47*(7), 650–654. https://doi.org/10.1130/G46219.1

Gomes, L., Miranda, H. S., Silvério, D. V., & Bustamante, M. M. C. (2020). Effects and behavior of experimental fires in grasslands, savannas, and forests of the Brazilian Cerrado. *Forest Ecology and Management*, *458*, 117804. https://doi.org/10.1016/j.foreco.2019.117804

Gorynski, K., & Mandel, R. (2009). Bioclimatic change inferred from the evolution of a late-quaternary alluvial fan in Western Kansas. In *Kansas Geological Survey Open File Report* (Vol. 21). Retrieved from http://www.kgs.ku.edu/Publications/OFR/2009/OFR09_21/index.html

Goudie, A. S., Allison, R. J., & McLaren, S. J. (1992). The relations between modulus of elasticity and temperature in the context of the experimental simulation of rock weathering by fire. *Earth Surface Processes and Landforms*, *17*(6), 605–615. https://doi.org/10.1002/esp.3290170606

Govers, G., & Poesen, J. (1998). Field experiments on the transport of rock fragments by animal trampling on scree slopes. *Geomorphology*, *23*(2), 193–203. https://doi.org/10.1016/S0169-555X(98)00003-8

Grab, S. W., Dickinson, K. J. M., Mark, A. F., & Maegli, T. (2008). Ploughing boulders on the Rock and Pillar Range, south-central New Zealand: Their geomorphology and alpine plant associations. *Journal of the Royal Society of New Zealand*, *38*(1), 51–70. https://doi.org/10.1080/03014220809510546

Hayden, B. P. (1998). Regional climate and the distribution of tallgrass prairie. In A. K. Knapp, J. M. Briggs, D. C. Hartnett, & S. L. Collins (Eds.), *Grassland dynamics: Long-term ecological research in tallgrass prairie* (pp. 19–34). Oxford University.

Hirano, M. (1968). A mathematical model of slope development: An approach to the analytical theory of erosional topography. *Journal of Geosciences Osaka City University*, *11*, 13–52.

Imbrie, J., Laporte, L. F., & Merriam, D. F. (1964). Beattie Limestone facies (Lower Permian) of the northern midcontinent. *Kansas Geological Survey Bulletin*, *169*, 219–238.

Johnson, W. C., Willey, K. L., & Macpherson, G. L. (2007). Carbon isotope variation in modern soils of the tallgrass prairie: Analogues for the interpretation of isotopic records derived from paleosols. *Quaternary International*, *162*(163), 3–20. https://doi.org/10.1016/j.quaint.2006.10.036

Johnstone, S. A., & Hilley, G. E. (2015). Lithologic control on the form of soil-mantled hillslopes. *Geology*, *43*(1), 83–86. https://doi.org/10.1130/g36052.1

Kalantari, B. (2012). Foundations on expansive soils: A review (Vol. *7*).

Knight, C. L., Briggs, J. M., & Nellis, M. D. (1994). Expansion of gallery forest on Konza Prairie research natural area, Kansas, USA. *Landscape Ecology*, *9*(2), 117–125.

Layzell, A. L., & Mandel, R. D. (2020). Late Quaternary landscape evolution and bioclimatic change in the central Great Plains, USA. *GSA Bulletin*, *132*(11–12), 2553–2571. https://doi.org/10.1130/B35462.1

Lee, X., Goulden, M. L., Hollinger, D. Y., Barr, A., Black, T. A., Bohrer, G., et al. (2011). Observed increase in local cooling effect of deforestation at higher latitudes. *Nature*, *479*(7373), 384–387. https://doi.org/10.1038/nature10588

Marston, R. A. (2010). Geomorphology and vegetation on hillslopes: Interactions, dependencies, and feedback loops. *Geomorphology*, *116*(3), 206–217. https://doi.org/10.1016/j.geomorph.2009.09.028

Martin, Y. (2000). Modelling hillslope evolution: Linear and nonlinear transport relations. *Geomorphology*, *34*(1–2), 1–21. https://doi.org/10.1016/s0169-555x(99)00127-0

Mccarroll, N., & Temme, A. (2022). RFP01 Properties of large hillslope blocks and cliff faces along the cottonwood limestone near the konza prairie nature trail [Dataset]. Environmental Data Initiative. https://doi.org/10.6073/pasta/65f917edea2318f7f7d63ae4239091c3

McFadden, L. D., Eppes, M. C., Gillespie, A. R., & Hallet, B. (2005). Physical weathering in arid landscapes due to diurnal variation in the direction of solar heating. *GSA Bulletin*, *117*(1–2), 161–173. https://doi.org/10.1130/B25508.1

McGrath, G. S., Nie, Z., Dyskin, A., Byrd, T., Jenner, R., Holbeche, G., & Hinz, C. (2013). In situ fragmentation and rock particle sorting on arid hills. *Journal of Geophysical Research: Earth Surface*, *118*(1), 17–28. https://doi.org/10.1029/2012JF002402

McLauchlan, K. K., Commerford, J. L., & Morris, C. J. (2013). Tallgrass prairie pollen assemblages in mid-continental North America. *Vegetation History and Archaeobotany*, *22*(3), 171–183. https://doi.org/10.1007/s00334-012-0369-8

Menting, F., Langston, A. L., & Temme, A. J. A. M. (2015). Downstream fining, selective transport, and hillslope influence on channel bed sediment in mountain streams, Colorado Front Range, USA. *Geomorphology*, *239*, 91–105. https://doi.org/10.1016/j.geomorph.2015.03.018

Oviatt, C. G. (1999). Geomorphology of Konza Prarie. *Journal of Environmental Quality*, *28*(5), 35–47.

Paronuzzi, P., & Serafini, W. (2009). Stress state analysis of a collapsed overhanging rock slab: A case study. *Engineering Geology*, *108*(1), 65–75. https://doi.org/10.1016/j.enggeo.2009.06.019

Pelletier, J. D., & Rasmussen, C. (2009). Quantifying the climatic and tectonic controls on hillslope steepness and erosion rate. *Lithosphere*, *1*(2), 73–80. https://doi.org/10.1130/L3.1

Pérez, F. L. (1985). Surficial talus movement in an Andean paramo of Venezuela. *Geografiska Annaler - Series A: Physical Geography*, *67*(3–4), 221–237. https://doi.org/10.1080/04353676.1985.11880148

Roering, J. J., Kirchner, J. W., & Dietrich, W. E. (1999). Evidence for nonlinear, diffusive sediment transport on hillslopes and implications for landscape morphology. *Water Resources Research*, *35*(3), 853–870. https://doi.org/10.1029/1998WR900090

Roering, J. J., Kirchner, J. W., Sklar, L. S., & Dietrich, W. E. (2001). Hillslope evolution by nonlinear creep and landsliding: An experimental study. *Geology*, *29*(2), 143–146. https://doi.org/10.1130/0091-7613(2001)029<0143:HEBNCA>2.0.CO;2

Román-Sánchez, A., Willgoose, G., Giráldez, J. V., Peña, A., & Vanwalleghem, T. (2019). The effect of fragmentation on the distribution of hillslope rock size and abundance: Insights from contrasting field and model data. *Geoderma*, *352*, 228–240. https://doi.org/10.1016/j.geoderma.2019.06.014

Roth, D. L., Doane, T. H., Roering, J. J., Furbish, D. J., & Zettler-Mann, A. (2020). Particle motion on burned and vegetated hillslopes. *Proceedings of the National Academy of Sciences of the United States of America*, *117*(41), 25335–25343. https://doi.org/10.1073/pnas.1922495117

Ruedrich, J., Bartelsen, T., Dohrmann, R., & Siegesmund, S. (2011). Moisture expansion as a deterioration factor for sandstone used in buildings. *Environmental Earth Sciences*, *63*(7–8), 1545–1564. https://doi.org/10.1007/s12665-010-0767-0

Schumm, S. A. (1967). Rates of surficial rock creep on hillslopes in Western Colorado. *Science*, *155*(3762), 560–562. https://doi.org/10.1126/science.155.3762.560

Shobe, C. M., Bennett, G. L., Tucker, G. E., Roback, K., Miller, S. R., & Roering, J. J. (2020). Boulders as a lithologic control on river and landscape response to tectonic forcing at the Mendocino triple junction. *GSA Bulletin*, *133*(3–4), 647–662. https://doi.org/10.1130/B35385.1

Shobe, C. M., Tucker, G. E., & Rossi, M. W. (2018). Variable-threshold behavior in rivers arising from hillslope-derived blocks. *Journal of Geophysical Research: Earth Surface*, *123*(8), 1931–1957. https://doi.org/10.1029/2017jf004575

Shobe, C. M., Turowski, J. M., Nativ, R., Glade, R. C., Bennett, G. L., & Dini, B. (2021). The role of infrequently mobile boulders in modulating landscape evolution and geomorphic hazards. *Earth-Science Reviews*, *220*, 103717. https://doi.org/10.1016/j.earscirev.2021.103717

Shtober-Zisu, N., & Wittenberg, L. (2021). Long-term effects of wildfire on rock weathering and soil stoniness in the Mediterranean landscapes. *Science of the Total Environment*, *762*, 143125. https://doi.org/10.1016/j.scitotenv.2020.143125

Smith, G. (1991). *Geomorphology and geomorphic history of the Konza Prairie research natural area, Riley and Geary counties, Kansas. Konza prairie LTER*. Kansas State University.

Szramek, K., Walter, L. M., Kanduč, T., & Ogrinc, N. (2011). Dolomite versus calcite weathering in hydrogeochemically diverse watersheds established on bedded carbonates (Sava and Soča Rivers, Slovenia). *Aquatic Geochemistry*, *17*(4), 357–396. https://doi.org/10.1007/s10498-011-9125-4

Temme, A. J. A. M., Armitage, J., Attal, M., van Gorp, W., Coulthard, T. J., & Schoorl, J. M. (2017). Developing, choosing and using landscape evolution models to inform field-based landscape reconstruction studies. *Earth Surface Processes and Landforms*, *42*(13), 2167–2183. https://doi.org/10.1002/esp.4162

Tucker, G. E., & Hancock, G. R. (2010). Modelling landscape evolution. *Earth Surface Processes and Landforms*, *35*(1), 28–50. https://doi.org/10.1002/esp.1952

Wells, T., Willgoose, G. R., & Hancock, G. R. (2008). Modeling weathering pathways and processes of the fragmentation of salt weathered quartz-chlorite schist. *Journal of Geophysical Research*, *113*(F1), F01014. https://doi.org/10.1029/2006JF000714